doi: 10.82124/CEAS-GNC-2026-079 CEAS-GNC-2026-079

EuroGNC Madrid, Spain May 5th-7th 2026

# Autonomous UAV Landing and Isolated Battery Recharging with Seamless Power Switching

**Ibrahim Khan** Department of Aerospace Engineering, Toronto Metropolitan University, Toronto, Canada. ibrahim1.khan@torontomu.ca

**Dennis Miklos** Department of Aerospace Engineering, Toronto Metropolitan University, Toronto, Canada. dmiklos@torontomu.ca

**Guangjun Liu** Department of Aerospace Engineering, Toronto Metropolitan University, Toronto, Canada. gjliu@torontomu.ca

*ABSTRACT*

**In this paper, we present an autonomous landing and recharging system with a proposed technique to electrically isolate the Unmanned Aerial Vehicle (UAV) battery during recharging while maintaining continuity of power to the UAV avionics. This ensures that the full charging current is directed solely to the battery - enabling safer recharging of the battery, while components such as the flight controller, companion computer, and other peripherals are continuously powered through a separate power path. We achieve this by developing a power distribution board (PDB) with integrated PowerPath controllers to seamlessly switch avionic loads from the onboard battery in the UAV to the charging source in the station without interruption upon docking. The overall system utilizes an omnidirectional station equipped with a contact-based interface and bidirectional communication to monitor and control the charging process. To support autonomous docking, a vision-based detection and localization approach is employed to ensure the precise alignment necessary for contact-based recharging. Experimental results have confirmed smooth power switching and consistent battery recharging.**

**Keywords:** UAV, Landing and Recharging Station, Autonomous Recharging, LiPo Battery, Battery Management System

## Nomenclature

| | | |
|---|---|---|
| $[t_x, t_y, t_z]$ | = | Translation Vector |
| $\mathcal{F}_W$ | = | World Frame |
| $\mathcal{F}_C$ | = | Camera Frame |
| $T$ | = | Transformation Matrix |
| $R$ | = | Rotation Matrix |
| $A$ | = | Area |

# 1 Introduction

Unmanned Aerial Vehicles (UAVs) have been applied in diverse applications but are constrained by limited battery capacity, which restricts flight duration, thus giving rise to autonomous recharging methods [1–3]. Contemporary work surrounding autonomous recharging includes wireless power transfer [4–6], Unmanned Ground Vehicles (UGVs) for recharging [7–9], contact-based charging [10] and battery swapping techniques [11–13]. Studies around autonomous UAV battery recharging show promising techniques for recharging, but do not isolate the battery from the electronic loads [14–17]. This means that the battery pack is in use by the onboard electronics, which complicates battery monitoring and the recharging process.

A number of studies provide evidence that charging a battery while it remains under load is comparable to charging under the influence of a current ripple effect [18–20]. The underlying mechanisms discussed in the literature, such as internal potential buildup, concentration polarization, and ripple-induced RMS current losses, indicate that these conditions reduce charging efficiency and accelerate battery aging. Specifically, ripple-like current oscillations have been shown to increase heating, worsen electrochemical stress, and promote chemical imbalances within the cell [20]. Since discharging and charging occur simultaneously when a battery is kept under load, the cell undergoes additional stress, which closely resembles the ripple charging profiles observed in prior research. These effects not only decrease coulombic efficiency but also accelerate capacity fade, thereby reducing the overall lifetime of the battery [21]. For this reason, our approach is focused on isolating the battery onboard the UAV while seamlessly offloading avionic load to a secondary source.

This paper presents a novel approach towards isolating the battery of the UAV and autonomously recharging it with a contact-based method. A custom-designed power distribution board (PDB) with a PowerPath controller is developed and implemented onboard for UAV hardware. The PDB electrically isolates the onboard battery of the UAV and continuously powers common components through a separate power path during docking and recharging. To demonstrate our work, we developed an omnidirectional docking station equipped with a passive-alignment mechanism. This system uses the UAV's own weight to guide it along a sliding surface, ensuring consistent and repeatable positioning for interfacing upon landing. Our work uniquely integrates autonomous landing and recharging into one comprehensive system, including battery isolation and routing of a separate power path, without any mechanical complexity or significant addition of weight. Our experiments show that integrating the PDB into the UAV produces similar charging curves to those obtained when the battery is directly connected to a recharger, ensuring no interference with avionics or efficiency loss compared to reported works. Finally, we validate the system's performance during autonomous flight operations, including takeoff, precise landing and recharging cycles without any power discontinuities.

The remainder of this paper is organized as follows: section 2 reviews related works on UAV charging stations; section 3 presents the methodology and design of the recharging station; section 4 covers controlled comparison of standalone and onboard recharging; section 5 covers flight experimentation, analysis of results and discussion; and finally, section 6 concludes the paper and outlines the direction of future work.

# 2 Related Works

This section reviews prior research on autonomous UAV battery recharging, emphasizing the various docking mechanisms employed and the degree to which battery isolation has been implemented.

## 2.1 Secondary Battery/Hot-Swapping

Hot-swapping refers to the replacement of a UAV's battery while maintaining continuous power to the avionics. A novel approach described in [22] employs a secondary drone to deliver a charged battery and perform an in-flight exchange with the depleted one, offering a robust solution for autonomous battery replacement, albeit without recharging the removed battery. In a related study [23], the authors propose autonomous battery recharging of a primary UAV using a secondary drone equipped with charging ports integrated into its landing gear. However, battery isolation is not implemented during the recharging process of the primary UAV in this configuration.

## 2.2 Unmanned Ground Vehicles

Air-ground collaboration with UAVs and UGVs is a developing field where the UGVs are equipped with charging interface on the roof of the vehicles. The UGVs are marked with features that can be identified and tracked by the UAV, which allows it to land on the pad for recharging [24]. The UGVs can be equipped with Wireless Power Transfer (WPT) pads [25, 26], contact charging pads [27] or a robotic arm to manually replace the battery altogether [28]. Despite being a promising technique to autonomously recharge UAV batteries, none of the studies isolate the battery prior to the commencement of recharging.

## 2.3 Omnidirectional Recharging

Recharging the UAV's battery regardless of its orientation makes the process less complicated by removing complex alignment fixing mechanisms. AutoCharge [15] uses a circular interface pattern to allow omnidirectional recharging functionality. To stabilize the recharging interface, AutoCharge proposes using Electro-Magnets (EMs) to secure the interfaces together and use convex-concave features to allow self-adjustment. Another study conducted on omnidirectional recharging used alternate polarized square copper areas along with contact terminals attached to the UAV's landing gear [14]. Omnidirectional recharging allows the UAV to relax precision when it is landing or performing orientation correction after landing.

## 2.4 Vision-based Autonomous UAV Landing

Vision-based autonomous landing for UAVs is a popular choice by mounting a downward-facing camera to observe the surface beneath because they are lightweight and inexpensive [29]. Computer vision strategies then enable precise touchdown on static or dynamic platforms, without the need for GPS. This is achieved by using a fiducial marker, a visually distinct reference point that is used to develop guidance systems to navigate the UAV towards a specific location. Many landing systems incorporate the use of AprilTags [30] or custom visual targets, with their tradeoff and details discussed in [31]. Recent research in this field is primarily focused on using deep learning, like the you-only-look-once (YOLO) model, to quickly detect the marker in varying environmental conditions [32, 33] or predicting errors from battery charge, flight path, altitude and velocity to correct the final landing position to enhance landing precision [34]. The challenge of these markers in real-world environments is that they occupy a large amount of space, especially when integrated within a recharge station. This often increases the overall size of the station, where active alignment systems are needed to align the UAV for recharging [35].

This section has highlighted different approaches to autonomous UAV battery recharging. The discussion has flying secondary battery systems, air-ground collaborations with UGVs, and omnidirectional recharging techniques. Building on this foundation, the following section delves into the methodology, presenting the core concepts and system overview, including the design of the landing station, interface, and onboard circuitry to further advance the proposed autonomous recharging solution.

# 3 System Architecture and Design

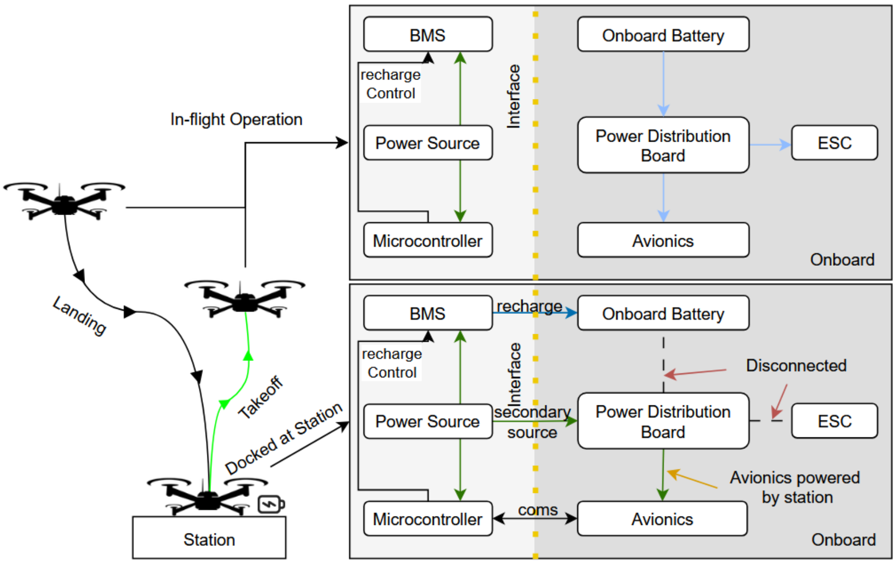


**Fig. 1 Power distribution onboard the UAV during in-flight operation and when docked at the station.**

This section introduces the core concept and design of the recharging system. The station in this work is developed to be compatible with a 4S LiPo battery and is detailed in the subsequent section. Inspired by the work of [15], the interface can be adapted to any LiPo battery by increasing the number of electrical connections and choosing the appropriate charger for balanced charging.

## 3.1 Electrical Design of the Power-Switching Architecture

The core framework of the power-switching and autonomous recharging is depicted in Fig. 1. A custom-designed PDB mounted on the UAV manages the transition from battery to ground power, ensuring uninterrupted operation of critical onboard systems such as the flight controller, onboard computer, ESCs, and camera module. To facilitate this process, a PowerPath controller - LTC 4416 [36], is installed on the PDB. The PDB accepts dual power inputs and distributes current through six parallel outputs, handling up to 50$A$ of current.

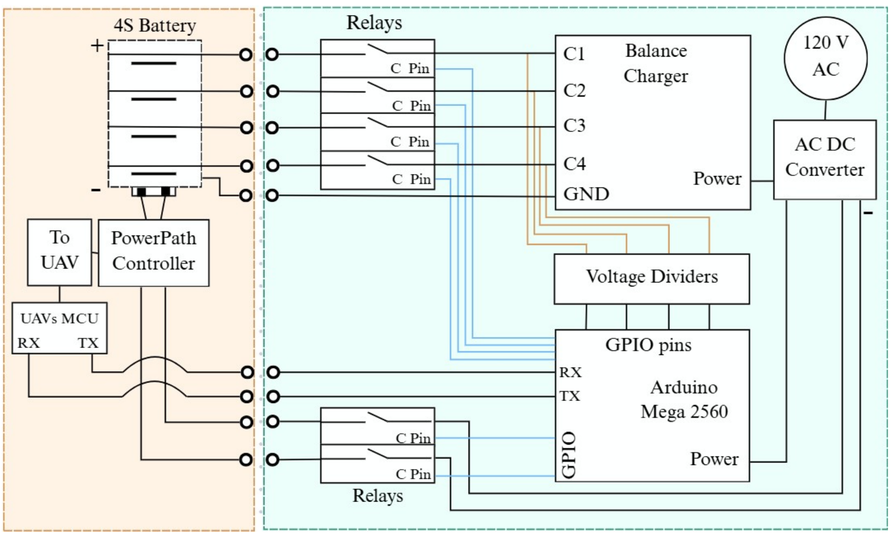


**Fig. 2 An illustrative diagram of the Recharging System.**

The integrated PDB automatically prioritizes the auxiliary power supply whose voltage is higher than the total battery pack voltage. When the auxiliary power is connected, the PDB powers the UAV system through ground power while simultaneously isolating the onboard battery for recharging. The working principle of the PDB achieving battery isolation is shown in Fig. 2. $Vout$ supplies power from either $V1$ or $V2$ to the avionics. When the PDB detects voltage input from the GS, it gives $V1$ priority and no longer registers $V2$, thereby isolating the battery. As the UAV switches to docking mode, the flight controller disarms the ESC by preventing the power supply to it from the battery.

## 3.2 Interface and Recharge Control

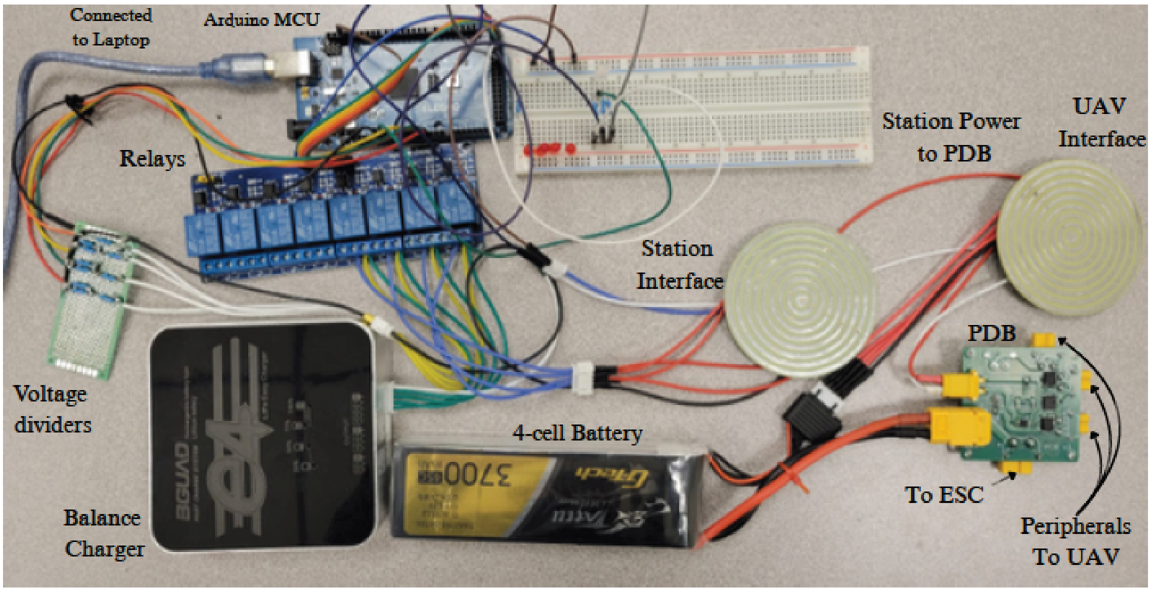


**Fig. 3 Component layout of the ground station and PDB connection**

The interface of the docking station sits at the center of the recharging station. The UAV and the ground station are both equipped with similar circular interfaces with 9 contact instances as shown in Fig. 3 with the wiring schematic in Fig. 2. Spring-loaded Pogo pins are used on the ground station as an interface to account for any possible discontinuity between the interfaces. The number of contact instances can be increased depending on the number of cells in the battery onboard the UAV. This work utilizes a 4-cell battery and hence, 9 instances are used: 2 pins for power transfer from the ground, 2 pins for UART communication and 5 pins for recharging.

When the UAV lands on the recharging station, a two-way serial communication link is established between the UAV and the ground station via UART to control the recharging process. After a successful docking, the MCU from the UAV communicates with the Arduino on the ground to activate the relays in a sequential manner. First, the ground power is connected to the PDB, which transitions the UAV avionics from battery power to ground power - which isolates the battery. Then, the relays associated with balance charging are activated, thus initiating the recharging process for an isolated battery. A dedicated 50 $W$ LiPo balance charger - BGUAD E4 is used to recharge the battery. A parallel connection from the balance leads is pulled to monitor the individual voltages. A voltage divider between the Arduino and the balance leads is used to reduce the magnitude of the voltage safe enough to be read by the Arduino. Conversely, to initiate a remote takeoff, the UAV's onboard computer commands the Arduino to deactivate the relays, switching the system back to battery power for continuous flight operations.

## 3.3 Recharge Station Design

The recharging station is developed with a catch bin, using a V-shaped cross-section that functions as a passive alignment mechanism with compatible landing gear. This unique shape will gently slide

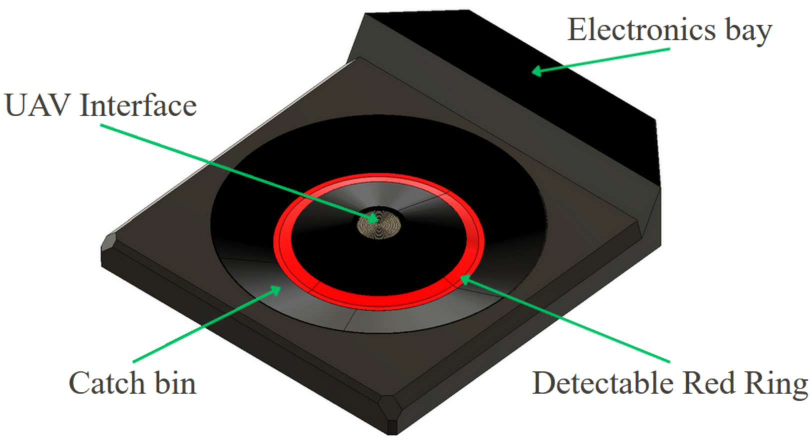


**Fig. 4 Recharge station design and layout.**

the UAV down the inclined surface under its own weight to the minimum point as illustrated in Fig. 4. By revolving the cross-section around the central axis, the catch bin can easily align with the UAV independent of its orientation. This is beneficial as it removes the need for precise orientation for contact-based charging. Fig. 5 shows the type-designed landing gear of the UAV, which matches the contours of the minimum point of the revolved cross-section and ensures proper alignment. A high-contrast red ring is embedded in the bottom of the catch bin. The colour red was chosen as it is easier to visually detect in different lighting conditions. We prototyped the station with a 3D printer using PLA as our choice of material since it generally has a low coefficient of friction [37]. Our design of the station included a catch bin with a slope of 20 °, capable of accommodating a landing error of ±10 cm from the center line. The V-shaped catch bin cross-section of the landing station is shown below.

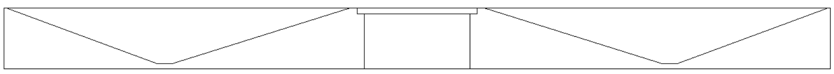

**Fig. 5 Layout and cross-section of station design.**

# 4 Comparison of Standalone and PDB Recharging

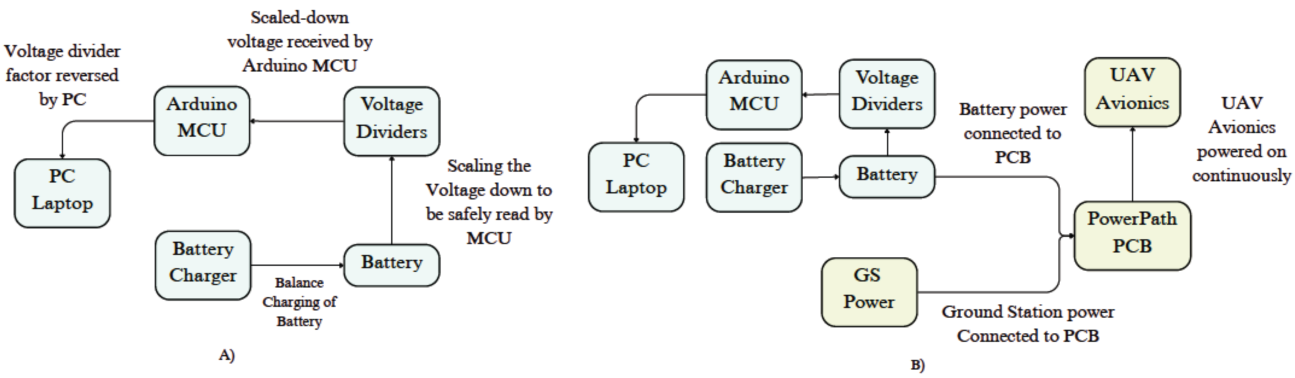


**Fig. 6 A) Setup configuration for simple UAV battery recharging. B) Configuration for UAV battery recharging with UAV avionics active via PDB.**

To validate the performance of the PDB, we conducted two sets of controlled experiments using a 4-cell LiPo battery with a capacity of 3700 mAh. Two tests were performed by standalone charging of the battery connected directly to the charger and compared with recharging via the the PDB with battery isolation at a) 3A and b) 5A with full UAV avionics active. The setup of this test is shown in Fig. 6. Prior to both tests, the LiPo battery was discharged at a constant rate of 1C until all individual cells reached a nominal voltage of 3.9 $V$. Since the balance charger used in this work does not output the charging curve of individual cells, we used an Arduino Micro-controller with a voltage divider circuit to sample and log the voltage of each individual cell every 0.5 seconds. We first gather a reference charging curve

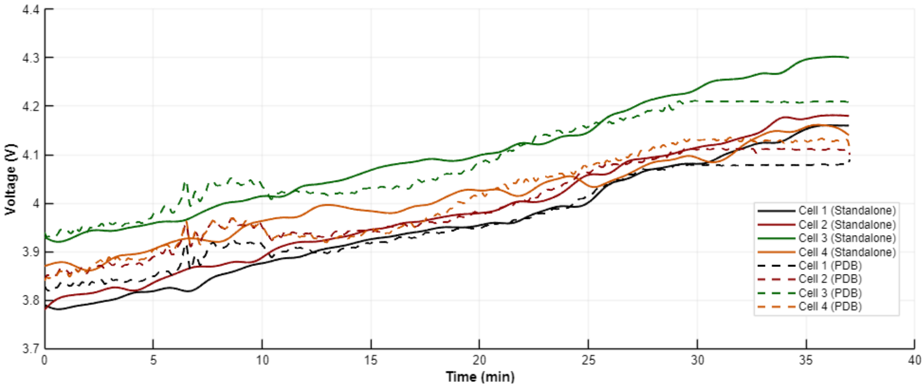


**Fig. 7 Individual cell voltages during recharging - standalone vs PDB with battery isolation at 3A.**

for both the tests, 3A and 5A, by directly charging the battery with the balance interface connected to the recharger, the voltage of individual cells in Fig. 7 and 9 obtained from standalone recharging is shown by the dashed lines.

Then we again discharged the same battery to a nominal cell voltage of 3.9 $V$ and configured the components as illustrated in Fig. 6 B). The XT60 connector of the battery was connected to the PDB onboard the UAV, which powered the avionics of the UAV. The flight computer was used to sense the output voltage from the PDB and log it at a frequency of 1 Hz. We note that from the input-to-output voltage across the PDB, there is a drop of 1.4 $V$ due to the high forward voltage introduced by the selected components for the PowerPath controller. The graph in Fig. 8 demonstrates the switching of the input voltage to the avionics once interfaced with the station.

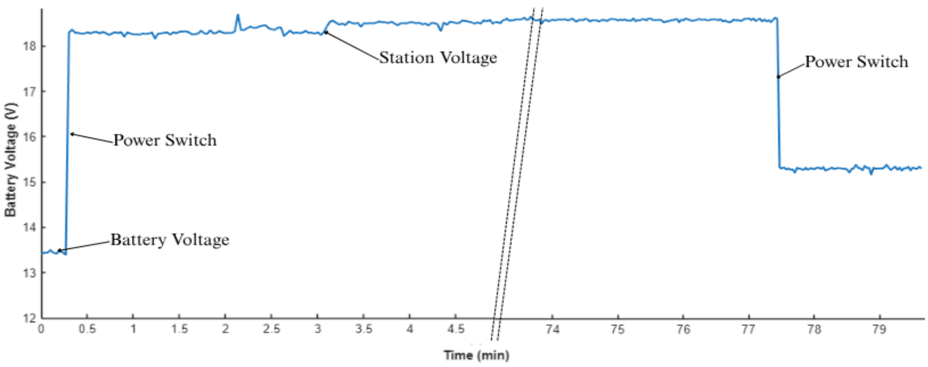


**Fig. 8 Voltage output from the PDB circuit as measured directly by the flight computer.**

At the beginning, the battery is the primary source for the avionics as seen by the 13.4 $V$. Once interfaced with the ground connector, the PowerPath controller in the PDB detects a higher input voltage to switch the voltage of the avionics to the station source of 18.2 $V$. The voltage change at the PDB's output indicates that the onboard electrical loads is seamlessly transitioned from battery power to the external supply. After isolating the battery, we activated the balanced charger via relays, and obtain the charging curves as shown in Fig. 9. By direct comparison to our reference charging curve, we notice that the recharging is comparable from a nominal cell voltage of 3.7 $V$ up to 4.2 $V$ for both scenarios. The total duration for the recharging process is 76.5 minutes with the PDB, a 30 second difference to our reference test. This demonstrates that the PDB effectively isolates the battery and directs all charging current to it, while the UAV avionics is powered by a secondary path and does not interfere.

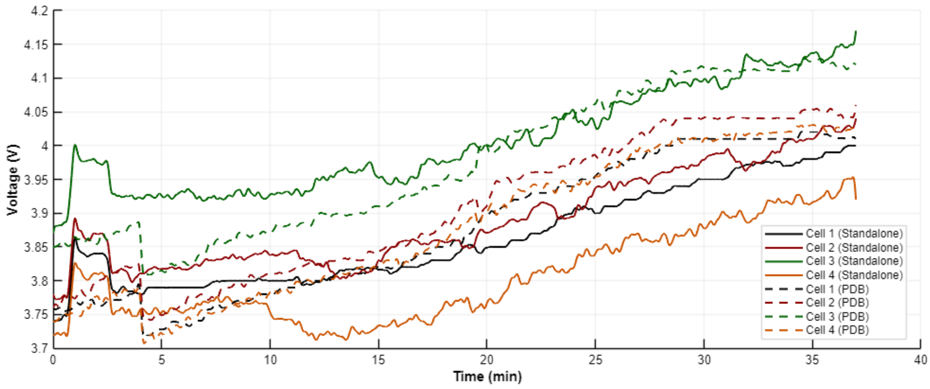


**Fig. 9 Individual cell voltages during recharging - standlone vs PDB with battery isolation at 5A.**

# 5 Autonomous Landing and Recharging Experiment

We validate our landing and recharge system with real-world indoor flight experiments in our flight laboratory. Our flight environment is 5 $m \times 5$ $m \times 3$ $m$ and equipped with the OptiTrack system, which provides localization information with an error 0.2 $mm$. This is used to describe the rigid-body transformation $T_B^W$ from the UAV body frame $\mathcal{F}_\mathcal{B}$, centred at the vehicle's IMU, to the world frame. We developed all algorithms in $C++$ and used the robotic operating system (ROS) for our implementation. Our flight tests are automated by a navigation script that will take off from the landing station, hover, and autonomously land on the station for recharging and subsequent takeoff. We detail the detection, localization and landing control in the subsequent sections.

## 5.1 Station Detection and Localization

The UAV detects the station by using a simple vision-based algorithm to recognize the red ring of the station using the OpenCV library [38]. The RGB image is converted into the hue-saturation-value (HSV) colour space, and pixels within the red hue range are isolated while applying lower bounds on saturation and value to reduce noise from low-intensity regions. The goal of the HSV model is to select the set of red pixels, then apply adaptive thresholding on their value component to enhance contour detection against varying illumination conditions. We utilize a hierarchy representation of the contours to find a pair that represents a ring feature. Each ring set is represented as a parent-child relationship, with the parent being the outer edge and the child being the inner edge. This effectively reduces the number of detected edges that can corresponding to the station. Each contour is then filtered based on its circularity, where a value of 1 represents a perfect circle, and as the value approaches 0, it represents irregular shapes:

$$circularity = \frac{4\pi A}{P^2} \tag{1}$$

where $A$ is the area of the contour and $P$ is the perimeter. If both outer and inner edges of the ring satisfy a circularity value of 0.9, the ring is detected and fitted with a bounding box. With the assumption that the camera is parallel to the station, the corner points of the box are used with the efficient Perspective-n-Point (EPNP) to estimate the translation vector $t^C = [t_x, t_y, t_z]$, where the superscript $C$ indicates the onboard UAV camera frame $\mathcal{F}_C$. Since our station does not resolve its orientation, the rotation vectors remain ambiguous and unused in this work.

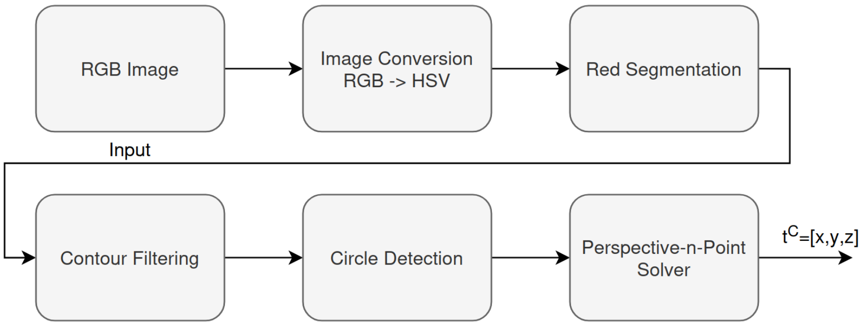


**Fig. 10 A flow chart of the Station Detection Pipeline.**

We leverage the transformation $T_C^W = T_B^W T_C^B$, describing the rigid-body transformation from the onboard camera frame to the world frame $\mathcal{F}_W$. Where $T_C^B$ is determined by using Kalibr, a camera-IMU calibration toolbox [39]. The transformation $T_C^W$ is composed of a rotation matrix $R_C^W \in SO(3)$ and a translation vector $t_C^W \in \mathbb{R}^3$, representing its position. This easily allows us to transform the stations point $t^C$ into the corresponding location in the world frame $t^W = [t'_x, t'_y, t'_z]$.

$$\begin{bmatrix} t'_x \\ t'_y \\ t'_z \\ 1 \end{bmatrix} = \begin{bmatrix} R_C^W & T_C^W \\ \mathbf{0}^{3\times1} & 1 \end{bmatrix} \begin{bmatrix} t_x \\ t_y \\ t_z \\ 1 \end{bmatrix} \tag{2}$$

The benefit of this approach is that regardless of how the UAV maneuvers, based on its observation of the station, its location in the world frame remains fixed.

## 5.2 Landing Control

Our subsystem for landing control leverages the stable world location of the station to ensure accurate positioning during the alignment and descent phase of the UAV. In case there are periodic failures in the detection, the control loop will utilize the last known world location, providing a steadier descent. The

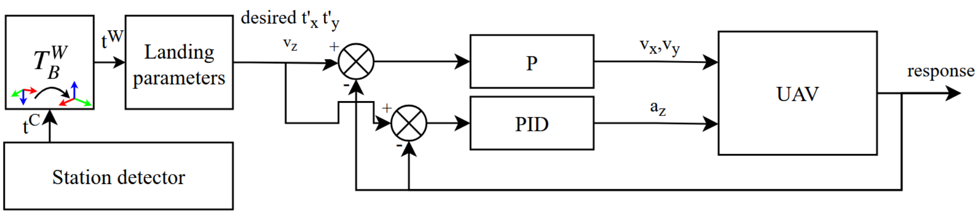


**Fig. 11 Structure of the landing controller.**

control loop employs a proportional controller to minimize the positional error and ensure the vehicle aligns with the target point $t'_x$ and $t'_y$, as shown in Fig. 11. The internal control architecture of the PX4 is used to generate velocity commands that guide the UAV towards the landing site. When the x-y error between the UAV and station is less than $\pm 5\ cm$, the UAV will descend with a velocity of $0.2\frac{m}{s}$ until touchdown.

## 5.3 Result and Discussion

In the conducted flight experiment shown in Fig. 12, the UAV initially rests on the ground station, drawing power from the ground supply through the station-UAV interface. With a remote command

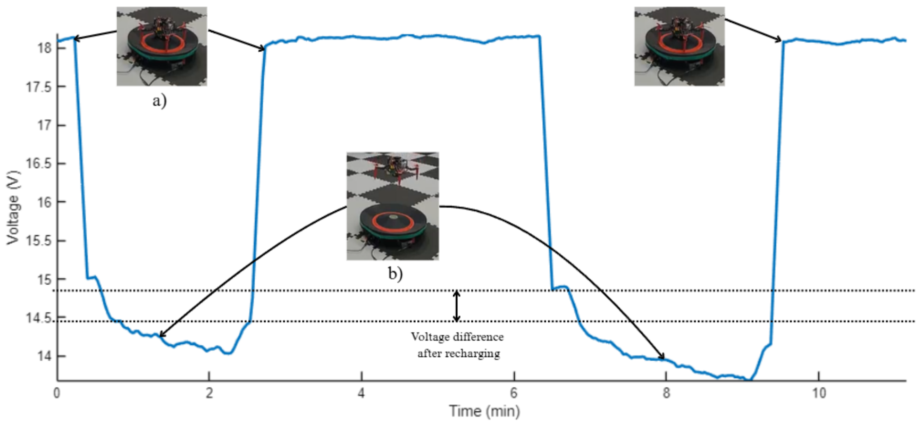


**Fig. 12 Flight test demonstration with take-off, landing, battery isolation and recharging. a) UAV is on the ground station with avionics powered on by the 18V power supply. b) UAV in flight, avionics powered by the onboard LiPo battery.**

to activate the takeoff, the onboard PDB transitions from ground power to the UAV's internal battery. Following a short-duration flight, the UAV returns to the docking station and autonomously lands based on the details in section 5.2. Post-landing, the UAV continues to operate on battery power until the docking procedure described in section 3.2 is fully completed. In this test, the battery was charged for a short duration (4 minutes) and the rise in the battery voltage is illustrated in Fig. 12. A remote command then re-initiates takeoff, which transitions the avionics back to the UAV's internal battery for the next flight cycle. This experiment validates the system's capability for applications that require continuous UAV operation across a repeated cycle of takeoff, flight, landing and recharging without operational interruptions or the need for human intervention.

While the proposed contact-based, battery-isolating recharging system demonstrated reliable operation in controlled indoor environments, several limitations remain. The conductive interface's reliance on spring-loaded pogo pins and exposed pads makes it sensitive to dust, debris, oxidation, and mechanical wear, which can increase contact resistance and intermittently disrupt charging or communication, necessitating periodic maintenance or replacement. The V-shaped passive catch bin also imposes minimum mass and geometry constraints, as lighter airframes or unconventional landing-gear designs may not generate sufficient normal force for firm electrical engagement, potentially reducing docking reliability without added compliance or active latching. Furthermore, the system's vision-based detection of the red landing ring is affected by lighting variations such as glare, shadows, or saturation, which can compromise perception robustness and landing precision despite short-term compensation through last-known pose estimates. Finally, scaling the PDB to support higher charge currents introduces thermal management challenges in the PCB, connectors, and charger circuitry, requiring enhanced cooling or heavier materials that could increase system size, weight, and cost.

Despite these limitations, the proposed system's architecture which features omnidirectional docking, battery isolation, and balance charging with cell-level monitoring enables several high-impact applications. In persistent indoor inspection and inventory tasks within warehouses, manufacturing floors, or research facilities, the system allows scheduled autonomous flights for sensing, or equipment checks. For security and safety patrols in environments such as data centers and transit hubs, the reliable power handover during docking ensures uninterrupted avionics operation for health diagnostics, log uploads, and software updates. The platform also serves as a valuable autonomous testbed for long-duration experiments in educational or research settings, supporting repeatable landings, consistent charge states, and minimal human supervision. Furthermore, in multi-robot operations, the station can function as a shared service node for staggered docking, data exchange and coordinated redeployment.

# 6 Conclusion

This paper presented the design and experimental validation of an autonomous landing and recharging system capable of electrically isolating the UAV battery during docking and recharging while maintaining continuous power to the avionics. The proposed architecture ensures that the full charging current is directed exclusively to the battery. A custom PDB with integrated PowerPath controllers was developed to seamlessly transfer the avionic load from the onboard battery to an auxiliary ground supply without interruption once docking occurs. The system incorporates an omnidirectional station with a contact-based electrical interface, providing reliable power transfer and real-time monitoring of the charging process. Experimental results verified smooth power switching, uninterrupted avionics operation during transition, and consistent battery recharging performance, confirming the effectiveness of the proposed isolation and power management technique. Collectively, these outcomes demonstrate a robust and efficient foundation for autonomous UAV recharging in indoor operational environments.

# Declaration of Use of Artificial Intelligence

Artificial intelligence (AI) tools were used solely for proofreading and language refinement purposes. Specifically - Grammarly, ChatGPT and Microsoft Editor were used to check grammar, sentence structure and vocabulary consistency.

# References


[1] Ali Bin Junaid, Aleksay Konoiko, Yahya Zweiri, M. Necip Sahinkaya, and Lakmal Seneviratne. Autonomous wireless self-charging for multi-rotor unmanned aerial vehicles. *Energies*, 10(6), 2017. ISSN: 1996-1073. doi: 10.3390/en10060803.

[2] T. Campi, S. Cruciani, F. Maradei, and M. Feliziani. Wireless charging system integrated in a small unmanned aerial vehicle (uav) with high tolerance to planar coil misalignment. In *2019 Joint International Symposium on Electromagnetic Compatibility, Sapporo and Asia-Pacific International Symposium on Electromagnetic Compatibility (EMC Sapporo/APEMC)*, pages 601–604, 2019. doi: 10.23919/EMCTokyo.2019.8893934.

[3] Yan Pan, Qianwu Chen, Nan Zhang, Zhigang Li, Ting Zhu, and Qingye Han. Extending delivery range and decelerating battery aging of logistics uavs using public buses. *IEEE Transactions on Mobile Computing*, 22(9):5280–5295, 2023. doi: 10.1109/TMC.2022.3167040.

[4] Steven Dunbar, Freeman Wenzl, Christopher Hack, Ronny Hafeza, Hasan Esfeer, Francois Defay, Sebastien Prothin, Damienne Bajon, and Zoya Popovic. Wireless far-field charging of a micro-uav. In *2015 IEEE Wireless Power Transfer Conference (WPTC)*, pages 1–4, 2015. doi: 10.1109/WPT.2015.7140154.

[5] Yuntao Wang, Zhou Su, Ning Zhang, and Ruidong Li. Mobile wireless rechargeable uav networks: Challenges and solutions. *IEEE Communications Magazine*, 60(3):33–39, 2022. doi: 10.1109/MCOM.001.2100731.

[6] Barathkumar T., Cyril Joshua J, Diwan Mohamed H, and Harish M. Fuzzy logic-based dynamic prioritization for uav wireless charging systems in agriculture. In *2024 International Conference on IoT Based Control Networks and Intelligent Systems (ICICNIS)*, pages 593–600, 2024. doi: 10.1109/ICICNIS64247.2024.10823327.

[7] Subramanian Ramasamy, Jean-Paul F. Reddinger, James M. Dotterweich, Marshal A. Childers, and Pranav A. Bhounsule. Cooperative route planning of multiple fuel-constrained unmanned aerial vehicles with recharging on an unmanned ground vehicle. In *2021 International Conference on Unmanned Aircraft Systems (ICUAS)*, pages 155–164, 2021. doi: 10.1109/ICUAS51884.2021.9476848.

[8] Lihua Ruan, Lingjie Duan, and Jianwei Huang. Optimal uav hitching on ground vehicles. In *2021 IEEE Global Communications Conference (GLOBECOM)*, pages 01–06, 2021. doi: 10.1109/GLOBECOM46510.2021.9685117.

[9] Ahmad Bilal Asghar, Guangyao Shi, Nare Karapetyan, James Humann, Jean-Paul Reddinger, James Dotterweich, and Pratap Tokekar. Risk-aware recharging rendezvous for a collaborative team of uavs and ugvs. In *2023 IEEE International Conference on Robotics and Automation (ICRA)*, pages 5544–5550, 2023. doi: 10.1109/ICRA48891.2023.10161446.

[10] Tommaso Addabbo, Stefano De Muro, Giacomo Falaschi, Ada Fort, Elia Landi, Riccardo Moretti, Marco Mugnaini, Francesco Nicolelli, Lorenzo Parri, Marco Tani, Marco Tesei, and Valerio Vignoli. An automatic battery recharge and condition monitoring system for autonomous drones. In *2020 IEEE International Workshop on Metrology for Industry 4.0 IoT*, pages 1–5, 2020. doi: 10.1109/MetroInd4.0IoT48571.2020.9138314.

[11] Yoad Guetta and Amir Shapiro. On-board physical battery replacement system and procedure for drones during flight. *IEEE Robotics and Automation Letters*, 7(4):9755–9762, 2022. doi: 10.1109/LRA.2022.3190077.

[12] Xiao Zhang and Lingjie Duan. Optimal patrolling trajectory design for multi-uav wireless servicing and battery swapping. In *2019 IEEE Globecom Workshops (GC Wkshps)*, pages 1–6, 2019. doi: 10.1109/GCWkshps45667.2019.9024535.

[13] Maggie Hoang, Alexander Ov, Shawn Chen, Don Huynh, Jose Vega, Nathan Kim, Yash Karwal, Steven Dobbs, and Zhen Yu. Design of autonomous battery swapping for uavs. In *2024 IEEE International Conference on Advanced Intelligent Mechatronics (AIM)*, pages 353–358, 2024. doi: 10.1109/AIM55361.2024.10637119.

[14] M.R. Al-Obaidi, M. A. Mustafa, Wan Zuha Wan Hasan, Norhafiz B. Azis, A. H. Sabry, S.P. Ang, and Zainidi Haji Abdul Hamid. Efficient charging pad for unmanned aerial vehicle based on direct contact. In *2018 IEEE 5th International Conference on Smart Instrumentation, Measurement and Application (ICSIMA)*, pages 1–5, 2018. doi: 10.1109/ICSIMA.2018.8688767.

[15] Alessandro Saviolo, Jeffrey Mao, Roshan Balu T M B, Vivek Radhakrishnan, and Giuseppe Loianno. Autocharge: Autonomous charging for perpetual quadrotor missions. In *2023 IEEE International Conference on Robotics and Automation (ICRA)*, pages 5400–5406, 2023. doi: 10.1109/ICRA48891.2023.10161503.

[16] N. Kemal Ure, Girish Chowdhary, Tuna Toksoz, Jonathan P. How, Matthew A. Vavrina, and John Vian. An automated battery management system to enable persistent missions with multiple aerial vehicles. *IEEE/ASME Transactions on Mechatronics*, 20(1):275–286, 2015. doi: 10.1109/TMECH.2013.2294805.

[17] Yuntao Wang, Zhou Su, Ning Zhang, and Ruidong Li. Mobile wireless rechargeable uav networks: Challenges and solutions. *IEEE Communications Magazine*, 60(3):33–39, 2022. doi: 10.1109/MCOM.001.2100731.

[18] Wiljan Vermeer, Marco Stecca, Gautham Ram Chandra Mouli, and Pavol Bauer. A critical review on the effects of pulse charging of li-ion batteries. In *2021 IEEE 19th International Power Electronics and Motion Control Conference (PEMC)*, pages 217–224, 2021. doi: 10.1109/PEMC48073.2021.9432555.

[19] David Muñoz-Torrero, Enrique García-Quismondo, Edgar Ventosa, Milan Prodanovic, and Jesús Palma. On the degradation of lithium-ion batteries over a current ripple effect. *Electrochimica Acta*, 530:146326, 2025. ISSN: 0013-4686. doi: https://doi.org/10.1016/j.electacta.2025.146326.

[20] Erik Goldammer, Marius Gentejohann, Michael Schlüter, Daniel Weber, Wolfgang Wondrak, Sibylle Dieckerhoff, Clemens Gühmann, and Julia Kowal. The impact of an overlaid ripple current on battery aging: The development of the sicwell dataset. *Batteries*, 8(2), 2022. ISSN: 2313-0105. doi: 10.3390/batteries8020011.

[21] Pablo Korth Pereira Ferraz and Julia Kowal. A comparative study on the influence of dc/dc-converter induced high frequency current ripple on lithium-ion batteries. *Sustainability*, 11(21), 2019. ISSN: 2071-1050. doi: 10.3390/su11216050.

[22] Yoad Guetta and Amir Shapiro. On-board physical battery replacement system and procedure for drones during flight. *IEEE Robotics and Automation Letters*, 7(4):9755–9762, 2022. doi: 10.1109/LRA.2022.3190077.

[23] Karan P. Jain and Mark W. Mueller. Flying batteries: In-flight battery switching to increase multirotor flight time. In *2020 IEEE International Conference on Robotics and Automation (ICRA)*, pages 3510–3516, 2020. doi: 10.1109/ICRA40945.2020.9197580.

[24] Khaled A. Ghamry, Yiqun Dong, Mohamed A. Kamel, and Youmin Zhang. Real-time autonomous take-off, tracking and landing of uav on a moving ugv platform. In *2016 24th Mediterranean Conference on Control and Automation (MED)*, pages 1236–1241, 2016. doi: 10.1109/MED.2016.7535886.

[25] Nansong Wu, Cristian Chacon, Zach Hakl, Kyle Petty, and Donny Smith. Design and implementation of an unmanned aerial and ground vehicle recharging system. In *2019 IEEE National Aerospace and Electronics Conference (NAECON)*, pages 163–168, 2019. doi: 10.1109/NAECON46414.2019.9058225.

[26] Yuntao Wang and Zhou Su. An envy-free online uav charging scheme with vehicle-mounted mobile wireless chargers. *China Communications*, 20(8):89–102, 2023. doi: 10.23919/JCC.fa.2023-0056.202308.

[27] Rashid Alyassi, Majid Khonji, Areg Karapetyan, Sid Chi-Kin Chau, Khaled Elbassioni, and Chien-Ming Tseng. Autonomous recharging and flight mission planning for battery-operated autonomous drones. *IEEE Transactions on Automation Science and Engineering*, 20(2):1034–1046, 2023. doi: 10.1109/TASE.2022.3175565.

[28] Éamon Barrett, Mark Reiling, Seyedmohsen Mirhassani, René Meijering, Jeroen Jager, Nicola Mimmo, Flavio Callegati, Lorenzo Marconi, Raffaella Carloni, and Stefano Stramigioli. Autonomous battery exchange of uavs with a mobile ground base. In *2018 IEEE International Conference on Robotics and Automation (ICRA)*, pages 699–705, 2018. doi: 10.1109/ICRA.2018.8460201.

[29] Cosimo Patruno, Massimiliano Nitti, Antonio Petitti, Ettore Stella, and Tiziana D'Orazio. A vision-based approach for unmanned aerial vehicle landing. *Journal of Intelligent & Robotic Systems*, 95(2):645–664, 2019. doi: 10.1007/s10846-018-0933-2.

[30] John Wang and Edwin Olson. Apriltag 2: Efficient and robust fiducial detection. In *2016 IEEE/RSJ International Conference on Intelligent Robots and Systems (IROS)*, pages 4193–4198. IEEE, 2016. doi: 10.1109/IROS.2016.7759617.

[31] Zahra Jafari-Shahbazzadeh and Alireza Binesh. Precision landing techniques for drones: A comprehensive review. *Iranian Journal of Science and Technology, Transactions of Mechanical Engineering*, pages 1–28, 2025. doi: 10.1007/s40997-025-00878-y.

[32] Lingxia Mu, Qingliang Li, Ban Wang, Youmin Zhang, Nan Feng, Xianghong Xue, and Wenzhe Sun. A vision-based autonomous landing guidance strategy for a micro-uav by the modified camera view. *Drones*, 7(6):400, 2023. doi: 10.3390/drones7060400.

[33] Paolo Veneruso, Enrico Miccio, Roberto Opromolla, Giancarmine Fasano, Giacomo Gentile, and Carlo Tiana. Vision-aided approach and landing through ai-based vertiport recognition*. In *2023 International Conference on Unmanned Aircraft Systems (ICUAS)*, pages 1270–1277, 2023. doi: 10.1109/ICUAS57906.2023.10155914.

[34] Rishik Bhandary, Balsam Alkouz, Babar Shahzaad, and Athman Bouguettaya. Predictive precision of enhanced drone landings. *Expert Systems with Applications*, 266:125830, 2025. ISSN: 0957-4174. doi: https://doi.org/10.1016/j.eswa.2024.125830.

[35] Carlo Giorgio Grlj, Nino Krznar, and Marko Pranjić. A decade of uav docking stations: A brief overview of mobile and fixed landing platforms. *Drones*, 6(1):17, 2022. doi: 10.3390/drones6010017.

[36] Linear Technology Corporation. *LTC4416/LTC4416-1: 36V, Low Loss Dual PowerPath Controllers for Large PFETs*. Milpitas, CA, USA, rev. a edition, July 2005. Datasheet.

[37] Şenol Şirin, Enes Aslan, and Gülşah Akincioğlu. Effects of 3d-printed pla material with different filling densities on coefficient of friction performance. *Rapid Prototyping Journal*, 29(1):157–165, 2023. doi: 10.1108/RPJ-03-2022-0081.

[38] G. Bradski. The OpenCV Library. *Dr. Dobb's Journal of Software Tools*, 2000.

[39] ETHZ ASL. Kalibr: Visual-inertial calibration toolbox. `https://github.com/ethz-asl/kalibr`, 2025.